

Multichannel Interpolation for Periodic Signals via FFT, Error Analysis and Image Scaling

Dong Cheng, Kit Ian Kou*

Abstract

This paper describes a new method for the multichannel interpolation of a discrete signal. It is shown that a bandlimited periodic signal f can be exactly reconstructed from finite samples of g_k ($1 \leq k \leq M$) which are the responses of M linear systems with input f . The proposed interpolation can also be applied to approximate non-bandlimited periodic signals. Quantitative error analysis is provided to ensure its effectiveness for approximating non-bandlimited periodic signals and its Hilbert transform. Importantly, involving the fast Fourier transform (FFT) computational technique, bring high computational efficiency and reliability of the proposed algorithm. The superior performance of the proposed algorithm is demonstrated by several simulations. Additionally, the proposed interpolation is applied to the image scaling problem. The empirical studies show that the proposed method performs better than the other conventional image scaling methods.

Keywords: Multichannel interpolation, sampling theorem, signal reconstruction, FFT, Hilbert transform, error analysis, image scaling.

1 Introduction

In practical applications, one often has a number of data points, obtained by sampling or experimentation, which represent the values of a continuous signal. Interpolation by simple functions (e.g., trigonometric functions or rational functions), as one of the important mathematical techniques used in physics and engineering sciences, deals with the problem of reconstructing or approximating the continuous signals from a series of discrete points. An ideal interpolation usually tells us that a continuous signal can be exactly and uniquely reconstructed from the discrete points if it satisfies some suitable conditions (e.g., bandlimited). Such an interpolation is also referred to as a sampling theorem in signal processing [1]. In general, sampling formulas interpolate the given data even if the specific conditions for perfect reconstruction cannot be met. The error analysis for interpolation or sampling formulas is of great importance because the continuous signals that need to be recovered do not satisfy the conditions for ideal interpolation in most circumstances. Due to the wide range applications of interpolation, finding new interpolation or sampling formulas with error estimations as well as developing their fast

algorithms for implementation have received considerable attentions in recently years (see e.g., [2, 3, 4, 5, 6, 7]).

Most of classical sampling formulas have centered around reconstructing a signal from its own samples [1, 6]. In fact, reconstructing a signal from data other than the samples of the original signal is possible. Papoulis [8] first proposed generalized sampling expansion (GSE) for bandlimited signals defined on real line \mathbb{R} . The GSE indicates that a σ -bandlimited signal f can be reconstructed from the samples of output signals of M linear systems. That is, one can reconstruct f from the samples $g_1(nT), \dots, g_M(nT)$ of the output signals

$$g_m(t) = \frac{1}{\sqrt{2\pi}} \int_{-\sigma}^{\sigma} F(\omega) H_m(\omega) e^{it\omega} d\omega, \quad m = 1, \dots, M$$

where F is Fourier transform of f and H_1, \dots, H_M are the system functions and $T = M\pi/\sigma$. The idea of GSE has been extended in different directions. Cheung [9] introduced GSE for real-valued multidimensional signals associated with Fourier transform, while Wei, Ran and Li [10, 11] presented the GSE with generalized integral transformation, such as fractional Fourier transform and linear canonical transform. In [12], the authors studied GSE for quaternion-valued signals associated with quaternion Fourier transform. Importantly, the applications based on GSE as well as its generalizations have been conducted by researchers [3, 13].

A finite duration signal is commonly assumed to be periodic in practice. Accordingly, there are certain studies concerning the interpolation theory of periodic signals. A sampling theorem for periodic signals was first introduced by Goldman [14]. The author in [15] proposed pseudo-orthogonal bases for reconstructing periodic signals. In a series of papers [16, 17, 18], researchers extensively discussed the sinc interpolation of discrete periodic signals and they also derived several equivalent interpolation formulas in distinct forms. As an extension of periodic sinc interpolation, decomposing a periodic signal in a basis of shifted and scaled versions of a generating function was studied in [19]. Moreover, they further presented an error analysis for their approximation method. Recently, the non-uniform sampling theorems for periodic signals were also presented [20, 21].

In this paper, a multichannel interpolation for periodic signals is studied. We derive a general interpolation formula that depends on the transfer functions of the linear systems. The formula bears a resemblance to the classical GSE defined on real line. Nevertheless, the recipe of derivation is different from the traditional one, and moreover, the proposed formula is given by a finite summation, as opposed to a infinite summation in the traditional case. The contributions of this paper are summarized as follows:

*Dong Cheng and Kit Ian Kou are with the Department of Mathematics, Faculty of Science and Technology, University of Macau, Macau (e-mail: chengdong720@163.com; kikou@umac.mo). The authors acknowledge financial support from the National Natural Science Foundation of China 11401606, University of Macau MYRG2015-00058-L2-FST and the Macao Science and Technology Development Fund FDCT/031/2016/A1.

1. We propose a multichannel interpolation for periodic signals (MIP). The proposed MIP is capable of generating various useful interpolation formulas by selecting suitable parameters according to the types and the amount of collected data. In addition, it would restore the original signal f and some integral transformations (such as Hilbert transform) of f .
2. A fast algorithm based on FFT is presented which brings high computational efficiency and reliability of the proposed algorithm of MIP.
3. To the authors' knowledge, there seems no error analysis for classical GSE in approximating general finite energy signal on real line in the literature. By contrast, we analyze the errors that arise in approximating non-bandlimited periodic signals by the proposed MIP.
4. The proposed MIP is applied to image scaling problem. Its main advantage makes good use of multifaceted information of image, so that the scaled image retains lots of information of the original unscaled image. The experimental simulations show the superiority of our method over the other three popularly used conventional methods: nearest neighbour, bilinear and bicubic.

The rest of the paper is organized as follows: Section 2 recalls some preliminaries of Fourier series. Section 3 formulates MIP and presents some examples to illustrate how to use MIP flexibly. The error analysis is drawn in Section 4. In Section 5, the effectiveness of the proposed MIP for approximating signals is demonstrated by several numerical examples and the application of MIP to image scaling is also addressed. Finally, conclusions are made in Section 6.

2 Preliminaries

This part recalls some preparatory knowledge of Fourier series (see e.g. [22]). Without loss of generality, we restrict attention to the 2π -periodic signals, or alternatively, we will consider the signals defined on unit circle \mathbb{T} .

Let $L^p(\mathbb{T})$ be the totality of functions such that

$$\|f\|_p := \left(\frac{1}{2\pi} \int_{\mathbb{T}} |f(t)|^p dt \right)^{\frac{1}{p}} < \infty.$$

For $f \in L^2(\mathbb{T}) \subset L^1(\mathbb{T})$, it can be written as

$$f(t) = \sum_{n \in \mathbb{Z}} a(n) e^{int} \quad (1)$$

with $\sum_{n \in \mathbb{Z}} |a(n)|^2 < \infty$, where the Fourier series is convergent to f in L^2 norm. It is well known that $L^2(\mathbb{T})$ is a Hilbert space with the inner product

$$(f, h) := \frac{1}{2\pi} \int_{\mathbb{T}} f(t) \overline{h(t)} dt, \quad \forall f, h \in L^2(\mathbb{T}).$$

If $f, h \in L^2(\mathbb{T})$ and their Fourier coefficients are respectively given by

$$f \sim a(n), \quad h \sim b(n).$$

By Hölder inequality, we have $\{a(n)b(n)\}, \{a(n)\overline{b(n)}\} \in l^1$ and the general version of Parseval's identity is of the form:

$$(f, h) = \sum_{n \in \mathbb{Z}} a(n) \overline{b(n)}.$$

Moreover, the convolution theorem gives

$$(f * h)(t) := \frac{1}{2\pi} \int_{\mathbb{T}} f(s) h(t-s) ds = \sum_{n \in \mathbb{Z}} a(n) b(n) e^{int}. \quad (2)$$

The analytic signal defined by the linear combination of original signal and its (circular) Hilbert transform is regarded as an useful representation from which the phase, energy and frequency may be estimated [23, 24]. The circular Hilbert transform [25, 26] for periodic signal f is given by

$$\begin{aligned} \mathcal{H}f(t) &= \sum_{n \in \mathbb{Z}} (-i \operatorname{sgn}(n)) a(n) e^{int} \\ &= \frac{1}{2\pi} \text{p.v.} \int_{\mathbb{T}} f(s) \cot\left(\frac{t-s}{2}\right) ds, \end{aligned}$$

where sgn is the signum function taking values 1, -1 or 0 for $n > 0$, $n < 0$ or $n = 0$ respectively. By definition, we have

$$\mathcal{H}^2 f(t) = -f(t) + a(0). \quad (3)$$

We will first concentrate on reconstruction problem of finite order trigonometric polynomials. To maintain consistent terminology with the classical case, in what follows, a finite order trigonometric polynomial is called a bandlimited signal. Specifically, a periodic signal $f(t)$ is said to be bandlimited if its sequence of Fourier coefficients possesses finite nonzero elements. Let $\mathbf{N} = (N_1, N_2) \in \mathbb{Z}^2$, in the sequel we denote by $B_{\mathbf{N}}$ the totality of bandlimited signals with the following form:

$$f(t) = \sum_{n \in I^{\mathbf{N}}} a(n) e^{int}, \quad I^{\mathbf{N}} = \{n : N_1 \leq n \leq N_2\}. \quad (4)$$

3 Formulation of MIP

Throughout the paper, let $N_1, N_2 \in \mathbb{Z}$, $M \in \mathbb{N}^+$ and assume that $N_2 - N_1 + 1$ is divisible by M , namely, $\frac{N_2 - N_1 + 1}{M} = L \in \mathbb{N}^+$. We cut the set of integers into pieces for convenience. Let us set

$$I_k = \{n : N_1 + (k-1)L \leq n \leq N_1 + kL - 1\}, \quad J_k = \bigcup_{l=k+1}^{M+k} I_l.$$

Then we have $I^{\mathbf{N}} = \bigcup_{k=1}^M I_k = J_0$ and $\mathbb{Z} = \bigcup_k I_k$.

For $1 \leq m \leq M$, let

$$h_m(t) = \sum_{n \in \mathbb{Z}} b_m(n) e^{int}, \quad (5)$$

$$g_m(t) = (f * h_m)(t) = \frac{1}{2\pi} \int_{\mathbb{T}} f(s) h_m(t-s) ds.$$

It follows from (2) that

$$g_m(t) = \sum_{n \in \mathbb{Z}} c_m(n) e^{int},$$

where $c_m(n) = a(n)b_m(n)$. We particularly mention that the series (5) may not be convergent in general. Nevertheless, $g_m(t)$ is well defined when $\{c_m(n)\} \in l^1$. In this case, $h_m(t)$ may be regarded as a distribution.

The proposed MIP is to reconstruct $f(t)$ from the samples of $g_1(t), g_2(t), \dots, g_M(t)$. To achieve this, it is naturally to expect that the simultaneous sampling of M signals will reduces sampling rate by $1/M$. we shall note that the signal expressed as Eq. (4) may be represented by a shorter length of summation as long as we introduce the following vectors.

For $n \in I_1$, let

$$\mathbf{A}_n = [a(n), a(n+L), a(n+2L), \dots, a(n+(M-1)L)],$$

$$\mathbf{E}_n(t) = [e^{int}, e^{i(n+L)t}, e^{i(n+2L)t}, \dots, e^{i(n+(M-1)L)t}]^T.$$

It follows that

$$f(t) = \sum_{n \in I^N} a(n)e^{int} = \sum_{n \in I_1} \sum_{k=0}^{M-1} a(n+kL)e^{i(n+kL)t}$$

$$= \sum_{n \in I_1} \mathbf{A}_n \mathbf{E}_n(t). \quad (6)$$

Similar considerations applying to $g_m(t)$, we have

$$g_m(t) = \sum_{n \in I_1} \mathbf{C}_{m,n} \mathbf{E}_n(t),$$

where

$$\mathbf{C}_{m,n} = [c(n), c(n+L), c(n+2L), \dots, c(n+(M-1)L)].$$

Owing to the periodicity of $\mathbf{E}_n(t)$, we easily obtain

$$\mathbf{E}_n\left(\frac{2\pi p}{L}\right) = e^{in\frac{2\pi p}{L}} [1, 1, \dots, 1]$$

for every $0 \leq p \leq L-1$. This leads to a simple expression for samples of $g_m(t)$, that is

$$g_m\left(\frac{2\pi p}{L}\right) = \sum_{n \in I_1} \mathbf{C}_{m,n} \mathbf{E}_n\left(\frac{2\pi p}{L}\right)$$

$$= \sum_{n \in I_1} e^{in\frac{2\pi p}{L}} \sum_{k=0}^{M-1} c_m(n+kL) \quad (7)$$

$$= \sum_{n \in I_1} d_m(n) e^{in\frac{2\pi p}{L}},$$

where $d_m(n) = \sum_{k=0}^{M-1} c_m(n+kL)$. The factor $e^{in\frac{2\pi p}{L}}$ gives us a hint that we may be able to express the samples of $g_m(t)$ in terms of the DFT matrix or its inverse matrix.

Lemma 1 Let $t_p = \frac{2\pi p}{L}$ and $\tilde{\mathbf{D}}_m = [d_m(N_1), d_m(N_1+1), \dots, d_m(N_1+L-1)]$. There is a matrix representation for samples of $g_m(t)$ in terms of the inverse DFT matrix. That is,

$$\frac{1}{L} [g_m(t_0), g_m(t_1), \dots, g_m(t_{L-1})] = \tilde{\mathbf{D}}_m \mathbf{F}_L^{-1} \mathbf{U}_L^{-1}, \quad (8)$$

where \mathbf{F}_L is the L -th order DFT matrix

$$\mathbf{F}_L = \begin{bmatrix} \omega^0 & \omega^0 & \omega^0 & \dots & \omega^0 \\ \omega^0 & \omega^1 & \omega^2 & \dots & \omega^{L-1} \\ \omega^0 & \omega^2 & \omega^4 & \dots & \omega^{2(L-1)} \\ \vdots & \vdots & \vdots & \ddots & \vdots \\ \omega^0 & \omega^{L-1} & \omega^{2(L-1)} & \dots & \omega^{(L-1)^2} \end{bmatrix} \quad (9)$$

with $\omega = e^{-2\pi i/L}$ and \mathbf{U}_L is a diagonal matrix

$$\mathbf{U}_L = \begin{bmatrix} \omega^0 & & & & \\ & \omega^{N_1} & & & \\ & & \omega^{2N_1} & & \\ & 0 & & \ddots & \\ & & & & \omega^{(L-1)N_1} \end{bmatrix}. \quad (10)$$

Proof. From Eq. (7), we can rewrite $g_m(t_p)$ as

$$\begin{bmatrix} d_m(N_1) \\ d_m(N_1+1) \\ \vdots \\ d_m(N_1+L-1) \end{bmatrix}^T \begin{bmatrix} e^{iN_1\frac{2\pi p}{L}} \\ e^{i(1+N_1)\frac{2\pi p}{L}} \\ \vdots \\ e^{i(L-1+N_1)\frac{2\pi p}{L}} \end{bmatrix}.$$

Note that $\omega = e^{-2\pi i/L}$, $\mathbf{U}_L^{-1} = \overline{\mathbf{U}_L}$ and $\mathbf{F}_L^{-1} = \frac{1}{L} \overline{\mathbf{F}_L}$, it follows that

$$\frac{1}{L} [e^{iN_1\frac{2\pi p}{L}}, e^{i(1+N_1)\frac{2\pi p}{L}}, \dots, e^{i(L-1+N_1)\frac{2\pi p}{L}}]^T$$

$$= \text{Product of } \mathbf{F}_L^{-1} \text{ and } (p+1)\text{-th column of } \mathbf{U}_L^{-1}.$$

Hence we immediately obtain Eq. (8) which completes the proof. \square

Following the definition of \mathbf{A}_n , for $n \in I_1$, we further set M by M matrix

$$\mathbf{H}_n = [b_k(n+jL-L)]_{jk}, \quad (11)$$

which means the jk element of \mathbf{H}_n is $b_k(n+jL-L)$. Suppose that \mathbf{H}_n is invertible for every $n \in I_1$ and we denote the inverse matrix as

$$\mathbf{H}_n^{-1} = \begin{bmatrix} q_{11}(n) & q_{12}(n) & \dots & q_{1M}(n) \\ q_{21}(n) & q_{22}(n) & \dots & q_{2M}(n) \\ \vdots & \vdots & \ddots & \vdots \\ q_{M1}(n) & q_{M2}(n) & \dots & q_{MM}(n) \end{bmatrix}.$$

Next we use the elements of \mathbf{H}_n^{-1} to construct the interpolation functions. Let

$$r_m(n) = \begin{cases} q_{mk}(n+L-kL), & \text{if } n \in I_k, k=1, 2, \dots, M, \\ 0 & \text{if } n \notin I^N, \end{cases} \quad (12)$$

and define

$$y_m(t) = \sum_{n \in I^N} r_m(n) e^{int}. \quad (13)$$

As with most conventional bandlimited interpolation methods, the interpolation functions of MIP are generated from some fixed functions by translations. The following result provides a matrix representation of shifted functions generated by $y_m(t)$.

Lemma 2 Let $t_p = \frac{2\pi p}{L}$ and $y_m(t)$ be defined by (13). The shifted functions of $y_m(t)$ can be expressed by

$$[y_m(t-t_0), y_m(t-t_1), \dots, y_m(t-t_{L-1})] = \tilde{\mathbf{V}}_m(t) \mathbf{F}_L \mathbf{U}_L \quad (14)$$

where $\mathbf{F}_L, \mathbf{U}_L$ are given respectively by (9), (10) and $\tilde{\mathbf{V}}_m(t)$ is defined as

$$\tilde{\mathbf{V}}_m(t) = [v_{m,N_1}(t), v_{m,N_1+1}(t), \dots, v_{m,L+N_1-1}(t)]$$

with $v_{m,n}(t) = \sum_{k=1}^M q_{mk}(n) e^{i(n+kL-L)t}$, for $n \in I_1$.

Proof. By the definition of y_m and rearranging the summation terms of Eq. (13), we get

$$\begin{aligned} & y_m(t - t_p) \\ &= \sum_{n \in I^N} r_m(n) e^{in(t - \frac{2\pi p}{L})} \\ &= \sum_{k=1}^M \sum_{n \in I_1} r_m(n + kL - L) e^{i(n+kL-L)(t - \frac{2\pi p}{L})} \\ &= \sum_{n \in I_1} \left(\sum_{k=1}^M r_m(n + kL - L) e^{i(n+kL-L)t} \right) e^{-in \frac{2\pi p}{L}}. \end{aligned}$$

From the piecewise defined $r_m(n)$ in Eq. (12), it is easy to verify that $r_m(n + kL - L) = q_{mk}(n)$ for all $n \in I_1$ and $1 \leq k \leq M$. It follows that $y_m(t - t_p)$ can be rewritten as

$$y_m(t - t_p) = \sum_{n \in I_1} v_{m,n}(t) e^{-in \frac{2\pi p}{L}}. \quad (15)$$

In view of the resemblance of Eq. (15) and Eq. (7) and by similar arguments to Lemma 1, we immediately have Eq. (14) which completes the proof. \square

Until now, in addition to representing the sampled values of $g_m(t)$ by $\tilde{\mathbf{D}}_m$, the interpolation functions $y_m(t - t_p)$ ($1 \leq m \leq M$, $0 \leq p \leq L - 1$) have been constructed from the elements of \mathbf{H}_n^{-1} . we shall now make a connection between $f(t)$ and $y_m(t - t_p)$. To achieve this, let

$$\begin{aligned} \mathbf{D}_n &= [d_1(n), d_2(n), d_3(n), \dots, d_M(n)], \\ \mathbf{V}_n(t) &= [v_{1,n}(t), v_{2,n}(t), v_{3,n}(t), \dots, v_{M,n}(t)]. \end{aligned}$$

By straightforward computations, we get

$$\mathbf{A}_n \mathbf{H}_n = \mathbf{D}_n, \quad (16)$$

$$\mathbf{H}_n [\mathbf{V}_n(t)]^T = \mathbf{E}_n(t). \quad (17)$$

Having introduced above notations, we are in position to show our main result which is referred to multichannel interpolation for periodic signals (MIP).

Theorem 1 Let $f \in B_N$ and g_m , \mathbf{H}_n be given above. If \mathbf{H}_n is invertible for all $n \in I_1$, then

$$f(t) = \frac{1}{L} \sum_{m=1}^M \sum_{p=0}^{L-1} g_m(t_p) y_m(t - t_p) \quad (18)$$

where $t_p = \frac{2\pi p}{L}$ and y_m is given by Eq. (13).

Proof. Multiplying Eq. (17) by \mathbf{A}_n and using Eq. (16), the expression (4) can be rewritten as

$$\begin{aligned} f(t) &= \sum_{n \in I_1} \mathbf{D}_n [\mathbf{V}_n(t)]^T = \sum_{n \in I_1} \sum_{m=1}^M d_m(n) v_{m,n}(t) \\ &= \sum_{m=1}^M \sum_{n \in I_1} d_m(n) v_{m,n}(t) = \sum_{m=1}^M \tilde{\mathbf{D}}_m [\tilde{\mathbf{V}}_m(t)]^T \\ &= \sum_{m=1}^M \tilde{\mathbf{D}}_m \mathbf{F}_L^{-1} \mathbf{U}_L^{-1} \mathbf{U}_L \mathbf{F}_L [\tilde{\mathbf{V}}_m(t)]^T \\ &= \frac{1}{L} \sum_{m=1}^M \sum_{p=0}^{L-1} g_m(t_p) y_m(t - t_p) \end{aligned} \quad (19)$$

The last equality is a consequence of Lemma 1 and 2. The proof is complete. \square

Remark 1 In general, \mathbf{H}_n has to be invertible for every $n \in I_1$ because the definition of $v_{m,n}(t)$ depends on $q_{mk}(n)$ ($1 \leq k \leq M$) which are the elements of \mathbf{H}_n^{-1} . However, if there is an index set $\Lambda \subset I_1$ such that $\mathbf{A}_n = \mathbf{0}$ for every $n \in \Lambda$, then \mathbf{H}_n is not necessary to be invertible for $n \in \Lambda$. This is due to the fact that the zero terms of (6) may be removed from the summation. In this case, we just need to set $q_{mk}(n) = 0$ ($1 \leq m, k \leq M$) for $n \in \Lambda$.

Now we use some examples to show how Theorem 1 can be flexibly used to derive various sampling formulas for periodic signals. For simplicity we shall restrict to the case where $N_2 = -N_1 = N$.

Example 1 We first present the most basic example for our results. Let $M = 1$, $t_p = \frac{2\pi p}{2N+1}$, $b(n) = 1$. By Theorem 1, we conclude that $f \in B_N$ can be recovered from its samples. That is,

$$f(t) = \frac{1}{2N+1} \sum_{p=0}^{2N} f(t_p) D_N(t - t_p) \quad (20)$$

where

$$D_N(t) = \begin{cases} \frac{\sin(\frac{1}{2} + N)t}{\sin \frac{1}{2}t}, & t \neq 2k\pi, \\ 2N+1 & t = 2k\pi; \end{cases}$$

is the N -th order Dirichlet kernel. This formula is referred to trigonometric interpolation for data $f(t_p)$ ($p = 0, 1, \dots, 2N$). It should be stressed that the interpolation formulas given in [16, 17, 18] are mathematically equivalent to Eq. (20). Note that the expression (20) is not numerically stable at which the function takes 0/0 form. Based on the DFT, the author in [17] obtained a numerically stable formulation which is somehow equivalent to interpolation by the FFT [27]. In fact, the DFT or FFT based expressions for trigonometric interpolation can be subsumed in Eq. (19).

Example 2 Theorem 1 permits us to express $f \in B_N$ from its samples and samples of its derivatives. Note that

$$f'(t) = \sum_{n \in I^N} i n a(n) e^{int}, \quad f''(t) = \sum_{n \in I^N} -n^2 a(n) e^{int}.$$

Let $g_1(t) = f(t)$, $g_2(t) = f'(t)$, $g_3(t) = f''(t)$, then \mathbf{H}_n should be defined by

$$\mathbf{H}_n = \begin{bmatrix} 1 & in & -n^2 \\ 1 & i(n+L) & -(n+L)^2 \\ 1 & i(n+2L) & -(n+2L)^2 \end{bmatrix}.$$

By straightforward computations,

$$\mathbf{H}_n^{-1} = \begin{bmatrix} \frac{2L^2 + 3Ln + n^2}{2L^2} & -\frac{n(2L+n)}{L^2} & \frac{n(L+n)}{2L^2} \\ \frac{i(3L+2n)}{2L^2} & -\frac{2i(L+n)}{L^2} & \frac{i(L+2n)}{2L^2} \\ -\frac{1}{2L^2} & \frac{1}{L^2} & -\frac{1}{2L^2} \end{bmatrix}.$$

In order to satisfy the assumption that $2N+1$ is divisible by $M = 3$, we have to assume that $N = 1 \pmod{3}$. Suppose that $N = 3N_0 + 1$, then $L = \frac{2N+1}{3} = 2N_0 + 1$. Consequently,

we obtain $v_{n,m}(t)$ as follows:

$$\begin{aligned} v_{1,n}(t) &= \frac{2L^2 + 3Ln + n^2}{2L^2} e^{int} - \frac{n(2L + n)}{L^2} e^{i(n+L)t} \\ &\quad + \frac{n(L + n)}{2L^2} e^{i(n+2L)t}, \\ v_{2,n}(t) &= \frac{i(3L + 2n)}{2L^2} e^{int} - \frac{2i(L + n)}{L^2} e^{i(n+L)t} \\ &\quad + \frac{i(L + 2n)}{2L^2} e^{i(n+2L)t}, \\ v_{3,n}(t) &= \frac{-1}{2L^2} e^{int} + \frac{1}{L^2} e^{i(n+L)t} - \frac{1}{2L^2} e^{i(n+2L)t}. \end{aligned}$$

By using $L = 2N_0 + 1$ and letting $p = 0$ in Eq. (15), we have that $y_1(t)$ equals

$$\frac{\sin^3((N_0 + \frac{1}{2})t) (N_0^2 + N_0 + 1 - (N_0 + 1)N_0 \cos t)}{(2N_0 + 1)^2 \sin^3(\frac{t}{2})}$$

and

$$\begin{aligned} y_2(t) &= \sum_{n \in I_1} v_{2,n}(t) = \frac{\sin(t) \sin^3((N_0 + \frac{1}{2})t)}{(2N_0 + 1)^2 \sin^3(\frac{t}{2})}, \\ y_3(t) &= \sum_{n \in I_1} v_{3,n}(t) = \frac{2 \sin^3((N_0 + \frac{1}{2})t)}{(2N_0 + 1)^2 \sin(\frac{t}{2})}. \end{aligned}$$

Note that for $b_m(n) = (in)^{m-1}$ ($1 \leq m \leq M$), the determinant of \mathbf{H}_n defined by (11) is a Vandermonde determinant. Therefore \mathbf{H}_n is invertible for all $n \in I_1$. This would imply that we can further derive a sampling formula for recovering f from its samples as well as the samples of its first $M - 1$ derivatives.

Having considered interpolation for the samples of original signal and its derivatives. We now continue to show how the samples of Hilbert transform of f can be used to reconstruct f itself. Interestingly, based on anti-involution property (3), MIP can be applied to compute Hilbert transform as well.

Example 3 Let $M = 1$ and $b(n) = -i \operatorname{sgn}(n)$. Note that $\mathbf{H}_n = b(n)$ does not satisfy the conditions of Theorem 1 because it is not invertible at $n = 0$. Nevertheless, By Remark 1, this inconsistency can be avoided if $a(0) = 0$. Since $b(n)^{-1} = i \operatorname{sgn}(n)$ for $n \neq 0$, then $y(t)$ equals

$$\sum_{0 < |n| \leq N} i \operatorname{sgn}(n) e^{int} = -2 \csc\left(\frac{t}{2}\right) \sin\left(\frac{Nt}{2}\right) \sin\left(\frac{1}{2}(1 + N)t\right)$$

and the sampling formula

$$\begin{aligned} f(t) &= \frac{-2}{2N+1} \sum_{p=0}^{2N} \mathcal{H}f(t_p) \csc\left(\frac{t-t_p}{2}\right) \\ &\quad \times \sin\left(\frac{N(t-t_p)}{2}\right) \sin\left(\frac{1+N}{2}(t-t_p)\right) \end{aligned} \quad (21)$$

holds if $f \in B_{\mathbf{N}}$ and $a(0) = 0$.

Note that $\mathcal{H}f(t) = \sum_{n \neq 0} (-i \operatorname{sgn}(n)) a_n e^{int}$ satisfies the preconditions for establishment of Eq. (21) inherently. By substituting f with $\mathcal{H}f$ in (21) and using (3), we conclude that the Hilbert transform of $f \in B_{\mathbf{N}}$ can be computed by

$$\begin{aligned} \mathcal{H}f(t) &= \frac{2}{2N+1} \sum_{p=0}^{2N} (f(t_p) - a(0)) \csc\left(\frac{t-t_p}{2}\right) \\ &\quad \times \sin\left(\frac{N(t-t_p)}{2}\right) \sin\left(\frac{1+N}{2}(t-t_p)\right). \end{aligned} \quad (22)$$

Unlike (21), the formula (22) is valid for the case of $a(0) \neq 0$. In fact, if $f \in B_{\mathbf{N}}$, we have

$$a(0) = \frac{1}{2\pi} \int_{\mathbb{T}} f(t) dt = \frac{1}{2N+1} \sum_{p=0}^{2N} f(t_p) \quad (23)$$

by direct computation.

Remark 2 Given a real-valued $(2N+1)$ -point discrete signal $\{x_r(p)\}$, $p = 0, 1, \dots, 2N$. By replacing $f(t_p)$ with $x_r(p)$ and letting $t = t_j = \frac{2\pi j}{2N+1}$, $j = 0, 1, \dots, 2N$ in the right hand side of (22), we get a discrete signal $x_i(j) = \mathcal{H}f(t_j)$. The DFT for $\{z(j) = x_r(j) + i x_i(j)\}$ is

$$Z(k) = \begin{cases} X(0), & k = 0, \\ 2X(k), & 1 \leq k \leq N, \\ 0, & N+1 \leq k \leq 2N, \end{cases}$$

where $X(\cdot)$ is the DFT of $x_r(\cdot)$. That means that x_i is the discrete Hilbert transform of x_r [28]. This fact reveals the relationship between discrete Hilbert transform and continuous circular Hilbert transform. For the discrete signal of even number, similar arguments can be made, we omit the details.

Example 4 The analytic signal associated with f is defined by $f_A(t) = f(t) + i \mathcal{H}f(t)$, it can be rewritten as

$$f_A(t) = \sum_{n=0}^N \widetilde{a}_n e^{int}$$

where $\widetilde{a}_n = a_n$ for $n = 0$ and $\widetilde{a}_n = 2a_n$ for $n \neq 0$. Applying Theorem 1 to $f_A(t)$, we have the following. If $f \in B_{\mathbf{N}}$, then

$$f(t) + i \mathcal{H}f(t) = \frac{1}{1+N} \sum_{p=0}^N (f(t_p) + i \mathcal{H}f(t_p)) y(t - t_p),$$

where $t_p = \frac{2\pi p}{N+1}$ and $y(t) = \sum_{n=0}^N e^{int} = y_r(t) + i y_i(t)$ with

$$y_r(t) = \csc\left(\frac{t}{2}\right) \cos\left(\frac{Nt}{2}\right) \sin\left(\frac{1}{2}(1+N)t\right)$$

and

$$y_i(t) = \csc\left(\frac{t}{2}\right) \sin\left(\frac{Nt}{2}\right) \sin\left(\frac{1}{2}(1+N)t\right).$$

Moreover, if f is real-valued, then

$$f(t) = \frac{1}{1+N} \sum_{p=0}^N f(t_p) y_r(t - t_p) - \mathcal{H}f(t_p) y_i(t - t_p), \quad (24)$$

$$\mathcal{H}f(t) = \frac{1}{1+N} \sum_{p=0}^N f(t_p) y_i(t - t_p) + \mathcal{H}f(t_p) y_r(t - t_p). \quad (25)$$

Example 5 In Example 4, we express f (or $\mathcal{H}f$) by the samples of f and $\mathcal{H}f$. However, the formulas (24) and (25) are only valid for the real-valued signals. By Theorem 1, it is natural to expect that we can deduce a new expression of f (resp. $\mathcal{H}f$) in terms of the samples of f and $\mathcal{H}f$ by letting $M = 2$, $b_1(n) = 1$, $b_2(n) = -i \operatorname{sgn}(n)$. Rewrite $f \in B_{\mathbf{N}}$ as $f(t) = \sum_{n=-N}^{N+1} a_n e^{int}$ with $a_{N+1} = 0$. Let $M = 2$, $L = N+1$ and $b_1(n) = 1$, $b_2(n) = -i \operatorname{sgn}(n)$. Then $g_1(t) = f(t)$, $g_2(t) = \mathcal{H}f(t)$ and

$$\mathbf{H}_n = \begin{bmatrix} 1 & -i \operatorname{sgn}(n) \\ 1 & -i \operatorname{sgn}(n+L) \end{bmatrix}.$$

It is clear that

$$\mathbf{H}_n^{-1} = \begin{bmatrix} \frac{1}{2} & \frac{1}{2} \\ -\frac{i}{2} & \frac{i}{2} \end{bmatrix} \quad \text{for } -N \leq n \leq -1, \quad \mathbf{H}_0^{-1} = \begin{bmatrix} 1 & 0 \\ -i & 1 \end{bmatrix}.$$

Then by definition (13), we get that

$$\begin{aligned} y_1(t) &= 1 + \sum_{n=-N}^{-1} \frac{1}{2} \left(e^{i(n+N+1)t} + e^{int} \right) \\ &= \frac{\cos((N+1)t) - \cos(Nt) + \cos(t) - 1}{2\cos(t) - 2}, \\ y_2(t) &= e^{i(N+1)t} - i - \frac{i(e^{-iNt} - 1)(e^{i(N+1)t} - 1)}{2(e^{it} - 1)}. \end{aligned}$$

Consequently, we obtain

$$f(t) = \frac{1}{1+N} \sum_{p=0}^N f(t_p) y_1(t - t_p) + \mathcal{H}f(t_p) y_2(t - t_p) \quad (26)$$

where $t_p = \frac{2\pi p}{N+1}$. Substituting f with $\mathcal{H}f$ in Eq. (26) and applying (3) again, we have that $\mathcal{H}f(t)$ equals

$$\frac{1}{1+N} \sum_{p=0}^N \mathcal{H}f(t_p) y_1(t - t_p) + (a(0) - f(t_p)) y_2(t - t_p). \quad (27)$$

The formulas (26) and (27) are applicable to complex-valued signals. By the similar arguments to (23), the value of $a(0)$ can be computed by the samples of f and $\mathcal{H}f$. Concretely,

$$a(0) = \frac{1}{1+N} \sum_{p=0}^N f(t_p) + i\mathcal{H}f(t_p) \quad (28)$$

holds for $f \in B_{\mathbf{N}}$.

Example 6 In Example 2, the problem of recovering f from its samples as well as the samples of its derivatives was studied. We are motivated by anti-involution property (3) to consider the problem of recovering $\mathcal{H}f$ from the samples of f along with its derivatives. We may use Theorem 1 to derive the sampling formula via finding the Fourier multipliers $b_1(n), b_2(n), b_3(n)$ for transforming $\mathcal{H}f$ to f, f', f'' . However, from Example 2, we may obtain a formula for reconstructing $\mathcal{H}f$ by taking Hilbert transform to $y_m(t - t_p)$ directly. To achieve this, by making use of (15) and the linearity of Hilbert transform, it suffices to obtain the Hilbert transform of $v_{m,n}(t)$ derived in Example 2. By invoking

$$\mathcal{H}\{e^{int}\} = -i \operatorname{sgn}(n) e^{int},$$

it is easy to get $\mathcal{H}\{v_{m,n}\}$ and therefore we can immediately obtain $\mathcal{H}\{y_m(\cdot - t_p)\}$. We omit the explicit expression of $\mathcal{H}\{y_m(\cdot - t_p)\}$ for its lengthiness.

Several examples have been presented to illustrate how to use the proposed MIP flexibly. In these examples, $I^{\mathbf{N}}$ is assumed to be symmetric to the origin for simplicity. For general $I^{\mathbf{N}}$, the expressions for $y_1(t), y_2(t), \dots, y_M(t)$ could be very complicated. Moreover the expressions for $y_1(t), y_2(t), \dots, y_M(t)$ (see Examples mentioned earlier), in general, are of 0/0 form at some points. In fact, we just need to compute $v_{1,n}(t), v_{2,n}(t), \dots, v_{M,n}(t)$ and then use the numerically stable expression (19) for implementation. It should be stressed that the expressions of

$v_{1,n}(t), v_{2,n}(t), \dots, v_{M,n}(t)$ would not change with $I^{\mathbf{N}}$ and the expression (19) could be computed cheaply by FFT.

Intensively, we have studied the formulas for approximating f or $\mathcal{H}f$. However, the applications of the proposed MIP go further than that. Generally speaking, it is applicable to the problem of reconstructing or approximating $\mathcal{Q}(f)$ from the samples of $\mathcal{Q}_1(f), \mathcal{Q}_2(f), \dots, \mathcal{Q}_M(f)$, where the operators \mathcal{Q} and $\mathcal{Q}_m, (1 \leq m \leq M)$ are determined by specific needs in practice.

4 Error analysis

In practice, the signals are not bandlimited in general. The errors for approximations by using the formulas derived in examples of the previous section occur naturally in applications. Therefore, it is rather important to estimate the errors that may arise in the practical applications when applying Theorem 1. In this section, f is merely assumed to be square integrable on unit circle and is not necessary to be bandlimited.

We define the following approximation operator:

$$\mathcal{T}_{\mathbf{N}}f(t) := \frac{1}{L} \sum_{m=1}^M \sum_{p=0}^{L-1} g_m\left(\frac{2\pi p}{L}\right) y_m\left(t - \frac{2\pi p}{L}\right). \quad (29)$$

Let $f_{\tau}(t) = f(t - \tau)$ denote the shifted signal. Note that

$$\mathcal{T}_{\mathbf{N}}f_{\tau}(t) = \frac{1}{L} \sum_{m=1}^M \sum_{p=0}^{L-1} g_m\left(\frac{2\pi p}{L}, \tau\right) y_m\left(t - \frac{2\pi p}{L}\right)$$

where

$$\begin{aligned} g_m\left(\frac{2\pi p}{L}, \tau\right) &= \frac{1}{2\pi} \int_{\mathbb{T}} f(\xi - \tau) h_m\left(\frac{2\pi p}{L} - \xi\right) d\xi \\ &= \sum_n a(n) b_m(n) e^{-in\tau} e^{in\frac{2\pi p}{L}}. \end{aligned} \quad (30)$$

It is easy to see that $\mathcal{T}_{\mathbf{N}}$ is not a shift-invariant operator, that means $\mathcal{T}_{\mathbf{N}}f(t - \tau) \neq \mathcal{T}_{\mathbf{N}}f_{\tau}(t)$ in general. The mean square error of approximation for f_{τ} is given by

$$\varsigma(f, \mathbf{N}, \tau) = \|f_{\tau} - \mathcal{T}_{\mathbf{N}}f_{\tau}\|_2^2 = \frac{1}{2\pi} \int_{\mathbb{T}} |f_{\tau}(t) - \mathcal{T}_{\mathbf{N}}f_{\tau}(t)|^2 dt.$$

Note that the period of signal 2π is divisible by $\frac{2\pi}{L}$ which is the spacing of the samples, it follows that $\varsigma(\tau, \mathbf{N})$ is $\frac{2\pi}{L}$ periodic in τ . The time shift τ may be regarded as the phase difference of f and f_{τ} . In most practical applications, the exact phase of signal is unknown [19]. Hence, we consider the following averaged error:

$$\varepsilon(f, \mathbf{N}) = \sqrt{\frac{L}{2\pi} \int_0^{\frac{2\pi}{L}} \varsigma(f, \mathbf{N}, \tau) d\tau}.$$

To state our results, we need to introduce two lemmas.

Lemma 3 Let $r_m(n)$ and $b_m(n)$ be given above. Then $\sum_{m=1}^M r_m(n) b_m(n) = 1$, for all $n \in I^{\mathbf{N}}$ and $\sum_{m=1}^M r_m(n_1) b_m(n_2) = 0$, for all $n_1, n_2 \in I^{\mathbf{N}}$ satisfying $\frac{n_1 - n_2}{L} \in \mathbb{Z} \setminus \{0\}$.

Lemma 4 Suppose that $\{a(n)b_m(n)\}_n \in l^1$ and let

$$z_{mn}(\tau) := \sum_k a(n+kL)b_m(n+kL)e^{-ikL\tau}.$$

Then $z_{mn}(\tau)$ is well-defined for every $n \in \mathbb{Z}$ and furthermore

$$z_{mn}(\tau) = \frac{e^{in\tau}}{L} \sum_{p=0}^{L-1} g_m\left(\frac{2\pi p}{L}, \tau\right) e^{-in\frac{2\pi p}{L}}. \quad (31)$$

Proof. Note that both sides of Eq. (31) are continuous, to prove Eq. (31), it suffices to verify that both sides possess the same Fourier series coefficients. We now need to compute

$$\frac{L}{2\pi} \int_0^{\frac{2\pi}{L}} \frac{e^{in\tau}}{L} \sum_{p=0}^{L-1} g_m\left(\frac{2\pi p}{L}, \tau\right) e^{-in\frac{2\pi p}{L}} e^{ikL\tau} d\tau.$$

Under the assumption of $\{a(n)b_m(n)\}_n \in l^1$, the series (30) converges uniformly in τ . Substituting $g_m(\frac{2\pi p}{L}, \tau)$ with the series representation and note that the uniform convergence permits the interchange of integral and infinite summation, we get that

$$\begin{aligned} & \frac{L}{2\pi} \int_0^{\frac{2\pi}{L}} \frac{e^{in\tau}}{L} \sum_{p=0}^{L-1} g_m\left(\frac{2\pi p}{L}, \tau\right) e^{-in\frac{2\pi p}{L}} e^{ikL\tau} d\tau \\ &= \frac{L}{2\pi} \int_0^{\frac{2\pi}{L}} \frac{e^{in\tau}}{L} \sum_{p=0}^{L-1} \sum_l a(l)b_m(l) e^{-il\tau} e^{il\frac{2\pi p}{L}} e^{-in\frac{2\pi p}{L}} e^{ikL\tau} d\tau \\ &= \frac{1}{L} \sum_{p=0}^{L-1} \sum_l a(l)b_m(l) e^{il\frac{2\pi p}{L}} e^{-in\frac{2\pi p}{L}} \frac{L}{2\pi} \int_0^{\frac{2\pi}{L}} e^{i(n+kL-l)\tau} d\tau \\ &= \frac{1}{L} \sum_{p=0}^{L-1} \sum_l a(l)b_m(l) e^{il\frac{2\pi p}{L}} e^{-in\frac{2\pi p}{L}} \delta(n+kL-l) \\ &= \frac{1}{L} \sum_{p=0}^{L-1} a(n+kL)b_m(n+kL) e^{i(n+kL)\frac{2\pi p}{L}} e^{-in\frac{2\pi p}{L}} \\ &= a(n+kL)b_m(n+kL). \end{aligned}$$

Here, $\delta(n) = 1$ if $n = 0$ and $\delta(n) = 0$ otherwise. \square

We now use the Parseval's identity to compute $\zeta(f, \mathbf{N}, \tau)$. By direct computations, we obtain the Fourier coefficients of f_τ and $\mathcal{T}_{\mathbf{N}}f_\tau$ respectively as $f_\tau \sim a(n)e^{-in\tau}$ and

$$\mathcal{T}_{\mathbf{N}}f_\tau \sim \frac{1}{L} \sum_{m=1}^M \sum_{p=0}^{L-1} g_m\left(\frac{2\pi p}{L}, \tau\right) e^{-in\frac{2\pi p}{L}} r_m(n).$$

By Lemma 4, we have $\mathcal{T}_{\mathbf{N}}f_\tau \sim e^{-in\tau} \sum_{m=1}^M r_m(n)z_{mn}(\tau)$. It follows that

$$\begin{aligned} & \frac{1}{2\pi} \int_{\mathbb{T}} |f_\tau(t)|^2 dt = \sum_{n \in \mathbb{Z}} |a(n)|^2, \\ & \frac{1}{2\pi} \int_{\mathbb{T}} \overline{f_\tau(t)} \mathcal{T}_{\mathbf{N}}f_\tau(t) dt = \sum_{n \in I^{\mathbf{N}}} \overline{a(n)} \sum_{m=1}^M r_m(n)z_{mn}(\tau), \quad (32) \end{aligned}$$

$$\frac{1}{2\pi} \int_{\mathbb{T}} |\mathcal{T}_{\mathbf{N}}f_\tau(t)|^2 dt = \sum_{n \in I^{\mathbf{N}}} \left| \sum_{m=1}^M r_m(n)z_{mn}(\tau) \right|^2. \quad (33)$$

Integrating both sides of Eq. (32) with respect to τ , we have that

$$\begin{aligned} & \frac{L}{2\pi} \int_0^{\frac{2\pi}{L}} d\tau \frac{1}{2\pi} \int_{\mathbb{T}} \overline{f_\tau(t)} \mathcal{T}_{\mathbf{N}}f_\tau(t) dt \\ &= \sum_{n \in I^{\mathbf{N}}} \overline{a(n)} \sum_{m=1}^M r_m(n) \frac{L}{2\pi} \int_0^{\frac{2\pi}{L}} z_{mn}(\tau) d\tau \\ &= \sum_{n \in I^{\mathbf{N}}} \overline{a(n)} \sum_{m=1}^M r_m(n) a(n) b_m(n) \\ &= \sum_{n \in I^{\mathbf{N}}} |a(n)|^2 \sum_{m=1}^M r_m(n) b_m(n) = \sum_{n \in I^{\mathbf{N}}} |a(n)|^2. \end{aligned} \quad (34)$$

Here we used the fact that $\frac{L}{2\pi} \int_0^{\frac{2\pi}{L}} z_{mn}(\tau) d\tau = a(n)b_m(n)$. The last equality is a consequence of $\sum_{m=1}^M r_m(n)b_m(n) = 1$. With the same arguments to Eq. (34), we have

$$\frac{L}{2\pi} \int_0^{\frac{2\pi}{L}} d\tau \frac{1}{2\pi} \int_{\mathbb{T}} f_\tau(t) \overline{\mathcal{T}_{\mathbf{N}}f_\tau(t)} dt = \sum_{n \in I^{\mathbf{N}}} |a(n)|^2.$$

By invoking the Parseval's identity again, for $1 \leq l, m \leq M$, we get that

$$\begin{aligned} & \frac{L}{2\pi} \int_0^{\frac{2\pi}{L}} z_{mn}(\tau) \overline{z_{ln}(\tau)} d\tau \\ &= \sum_{k \in \mathbb{Z}} a(n+kL)b_m(n+kL) \overline{a(n+kL)b_l(n+kL)} \\ &= \sum_{k \in \mathbb{Z}} |a(n+kL)|^2 b_m(n+kL) \overline{b_l(n+kL)}. \end{aligned}$$

Therefore by integrating both sides of Eq. (33) with respect to τ , we get that

$$\begin{aligned} & \int_0^{\frac{2\pi}{L}} d\tau \frac{1}{2\pi} \int_{\mathbb{T}} |\mathcal{T}_{\mathbf{N}}f_\tau(t)|^2 dt \\ &= \int_0^{\frac{2\pi}{L}} d\tau \sum_{n \in I^{\mathbf{N}}} \sum_{m=1}^M \sum_{l=1}^M r_m(n) \overline{r_l(n)} z_{mn}(\tau) \overline{z_{ln}(\tau)} \\ &= \sum_{n \in I^{\mathbf{N}}} \sum_{m=1}^M \sum_{l=1}^M r_m(n) \overline{r_l(n)} \sum_{k \in \mathbb{Z}} |a(n+kL)|^2 \\ & \quad \times b_m(n+kL) \overline{b_l(n+kL)} \\ &= \sum_{k \in \mathbb{Z}} \sum_{n \in I^{\mathbf{N}}} |a(n+kL)|^2 \left| \sum_{m=1}^M r_m(n) b_m(n+kL) \right|^2. \end{aligned} \quad (35)$$

By a change of variables and note that $J_k = \bigcup_{l=k+1}^{M+k} I_l$, Eq. (35) can be rewritten as

$$\sum_{k \in \mathbb{Z}} \sum_{n \in J_k} |a(n)|^2 \left| \sum_{m=1}^M r_m(n-kL) b_m(n) \right|^2.$$

From Lemma 3, we have that

$$\sum_{n \in J_0} |a(n)|^2 \left| \sum_{m=1}^M r_m(n) b_m(n) \right|^2 = \sum_{n \in I^{\mathbf{N}}} |a(n)|^2$$

and

$$\sum_{k \neq 0} \sum_{n \in J_k \cap I^{\mathbf{N}}} |a(n)|^2 \left| \sum_{m=1}^M r_m(n-kL) b_m(n) \right|^2 = 0.$$

$$\begin{aligned}\varepsilon(f, \mathbf{N})^2 &= \sum_{n \in \mathbb{Z}} |a(n)|^2 - 2 \sum_{n \in I^{\mathbf{N}}} |a(n)|^2 + \sum_{n \in I^{\mathbf{N}}} |a(n)|^2 + \sum_{k \notin \{1, 2, \dots, M\}} \sum_{n \in I_k} |a(n)|^2 \sum_{l=1}^M \left| \sum_{m=1}^M r_m(n + (l-k)L) b_m(n) \right|^2 \\ &= \sum_{n \notin I^{\mathbf{N}}} |a(n)|^2 + \sum_{k \notin \{1, 2, \dots, M\}} \sum_{n \in I_k} |a(n)|^2 \sum_{l=1}^M \left| \sum_{m=1}^M r_m(n + (l-k)L) b_m(n) \right|^2\end{aligned}\quad (36)$$

$$\begin{aligned}&\leq \sum_{n \notin I^{\mathbf{N}}} |a(n)|^2 + \sum_{n \notin I^{\mathbf{N}}} |a(n)|^2 \left(\sum_{m=1}^M |b_m(n)|^2 \right) \sum_{l=1}^M \left(\sum_{k=1}^M |\Omega_k(L)|^2 \right) \\ &= \sum_{n \notin I^{\mathbf{N}}} |a(n)|^2 + \sum_{n \notin I^{\mathbf{N}}} \sum_{m=1}^M |a(n) b_m(n)|^2 M \left(\sum_{k=1}^M |\Omega_k(L)|^2 \right).\end{aligned}\quad (37)$$

Then Eq. (35) reduces to

$$\sum_{n \in I^{\mathbf{N}}} |a(n)|^2 + \sum_{k \neq 0} \sum_{n \in J_k - I^{\mathbf{N}}} |a(n)|^2 \left| \sum_{m=1}^M r_m(n - kL) b_m(n) \right|^2.$$

Rearranging the terms, the second part of the above equation becomes

$$\sum_{k \notin \{1, 2, \dots, M\}} \sum_{n \in I_k} |a(n)|^2 \sum_{l=1}^M \left| \sum_{m=1}^M r_m(n + (l-k)L) b_m(n) \right|^2.$$

Combining the computations above, $\frac{L}{2\pi} \int_0^{\frac{2\pi}{L}} \varsigma(f, \mathbf{N}, \tau) d\tau$ (namely $\varepsilon(f, \mathbf{N})^2$) can be expressed as Eq. (36).

Theorem 2 *Let $f \in L^2(\mathbb{T})$, then the expression of $\varepsilon(f, \mathbf{N})$ is given by square root of Eq. (36).*

Let $\mu(I^{\mathbf{N}}) = LM$ denotes the total number of elements of $I^{\mathbf{N}}$. For fixed M and b_1, b_2, \dots, b_M , roughly speaking, $\varepsilon(f, \mathbf{N})$ tends to 0 as $\mu(I^{\mathbf{N}}) \rightarrow \infty$ (or $L \rightarrow \infty$) if the rate of $|a(n)b_m(n)| \rightarrow 0$ is sufficiently fast as $|n| \rightarrow \infty$. There are no unified conditions to ensure $\varepsilon(f, \mathbf{N}) \rightarrow 0$ as $\mu(I^{\mathbf{N}}) \rightarrow \infty$, it should be concretely analyzed for the different situations. This is due to the fact that $r_m(n)$ is constructed from \mathbf{H}_n^{-1} which depends on $\mu(I^{\mathbf{N}})$ (or L). Nevertheless, a rough estimation can be given for Eq. (36). For $1 \leq m \leq M$, let

$$\Omega_m(b_1, b_2, \dots, b_M, \mu(I^{\mathbf{N}})) = \sup_{i \in I^{\mathbf{N}}} |r_m(i)|^2.$$

Keeping in mind that Ω_m is dependent on b_1, b_2, \dots, b_M , we may rewrite the above equation as

$$\Omega_m(L) = \sup_{i \in I^{\mathbf{N}}} |r_m(i)|^2$$

for simplicity. Applying Cauchy-Schwarz inequality to Eq. (36), it follows that the value of $\varepsilon(f, \mathbf{N})^2$ is bounded by Eq. (37).

Suppose that there exists a constant $C_1 > 0$ such that

$$\sum_{m=1}^M |\Omega_m(L)|^2 \leq C_1 L^\alpha$$

for all large L . Then $\varepsilon(f, \mathbf{N}) \rightarrow 0$ as $L \rightarrow \infty$ if there exists $C_2 > 0$ and $\beta < \min\{-1, -\alpha - 1\}$ such that

$$|a(n)b_m(n)|^2 \leq C_2 |n|^\beta, \quad 1 \leq m \leq M$$

for all large $|n|$. By invoking Eq. (12), we have

$$\Omega_m(L) = \sup_{1 \leq j \leq M, i \in I_1} |q_{mj}(i)|^2.$$

For Example 2, note that the factor L^2 in the denominators of \mathbf{H}_n^{-1} , it is not difficult to see that $\Omega_1(L)$ is bounded with respect to L , and $\Omega_2(L), \Omega_3(L)$ tend to 0 as $L \rightarrow \infty$. Therefore there exists a constant $C_1 > 0$ such that $\sum_{m=1}^3 |\Omega_m(L)|^2 \leq C_1$ for all L . For Example 5, $\Omega_1(L), \Omega_2(L)$ are independent on L , it is obvious that $\sum_{m=1}^2 |\Omega_m(L)|^2$ is bounded with respect to L .

If $f \in B_{\mathbf{N}}$, the proposed MIP (18) can perfectly reconstruct f by Theorem 1. This fact is also reflected in Eq. (36), namely $\varepsilon(f, \mathbf{N}) = 0$ if $a(n) = 0$ for all $n \notin I^{\mathbf{N}}$. It means that if $f \in B_{\mathbf{N}}$, whatever M and b_1, b_2, \dots, b_M we select, the approximation operator $\mathcal{T}_{\mathbf{N}} f$ defined by (29) will come into being the same result provided that the total samples used in Eq. (29) is equal to $\mu(I^{\mathbf{N}})$. In general, however, for fixed $\mu(I^{\mathbf{N}})$, it follows from Eq. (36) that different M and b_1, b_2, \dots, b_M for $\mathcal{T}_{\mathbf{N}} f$ may lead to different results if $f \notin B_{\mathbf{N}}$. We can also see this from the numerical examples in the next section.

5 Numerical examples and applications

5.1 Numerical examples

In this part, we shall demonstrate the effectiveness of $\mathcal{T}_{\mathbf{N}}$ for approximating signals experimentally. We compare the results by using the different formulas derived in Section 3 for approximating of f (or $\mathcal{H}f$). Let

$$\phi(z) = \frac{0.08z^2 + 0.06z^{10}}{(1.3 - z)(1.5 - z)} + \frac{0.05z^3 + 0.09z^{10}}{(1.2 + z)(1.3 + z)}.$$

From the theory of Hardy space, the imaginary part of $\phi(e^{it})$ is the Hilbert transform of its real part. In the following we select $f(t) = \Re[\phi(e^{it})]$, then its Hilbert transform is $\mathcal{H}f(t) = \Im[\phi(e^{it})]$.

The relative error for approximating f is defined by

$$\begin{aligned}\delta_1 &= \left(\sum_{p=0}^{2047} |f(t_p) - \mathcal{T}_{\mathbf{N}} f(t_p)|^2 \right)^{\frac{1}{2}} \bigg/ \left(\sum_{p=0}^{2047} |f(t_p)|^2 \right)^{\frac{1}{2}} \\ &\approx \left(\int_{\mathbb{T}} |f(t) - \mathcal{T}_{\mathbf{N}} f(t)|^2 dt \right)^{\frac{1}{2}} \bigg/ \left(\int_{\mathbb{T}} |f(t)|^2 dt \right)^{\frac{1}{2}}\end{aligned}$$

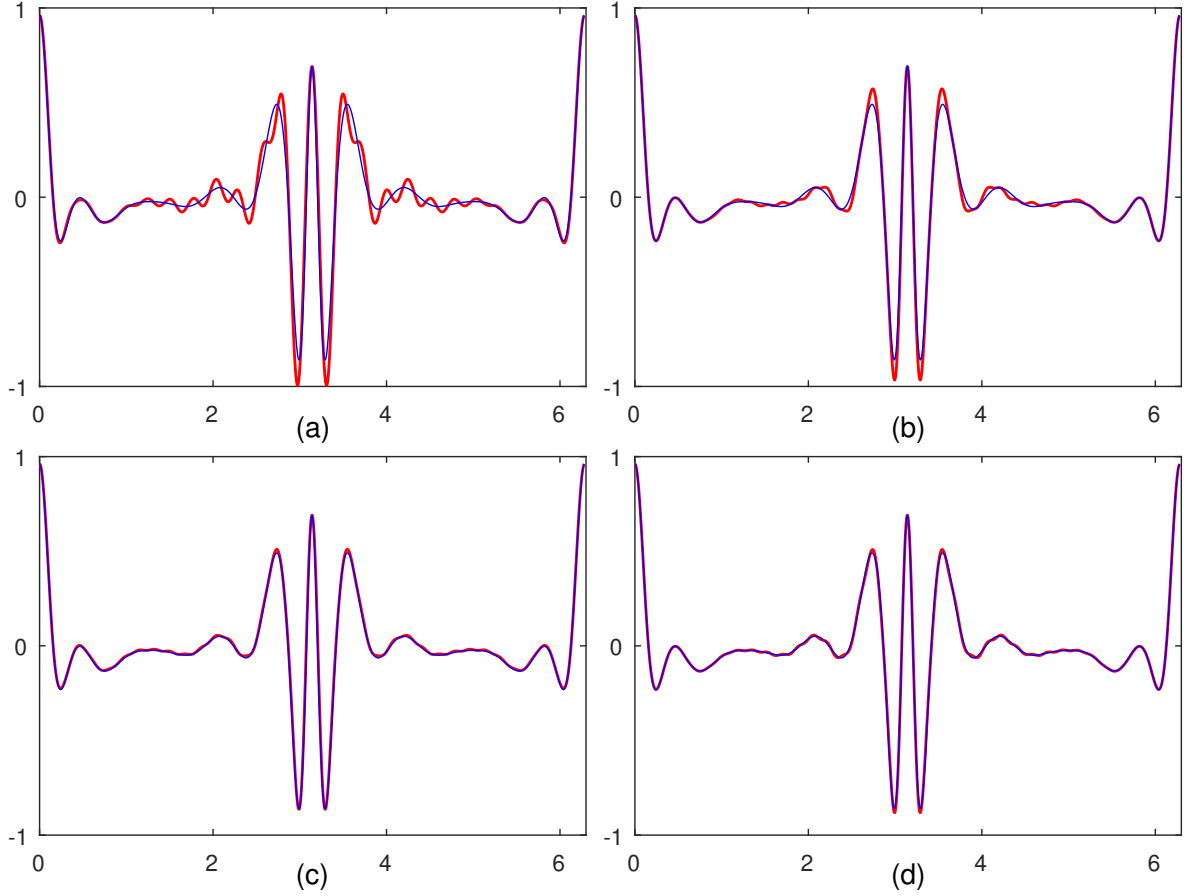


Figure 1: The blue line is the actual f . The red lines are approximated results for f by using (a) 48 samples of f ; (b) 24 samples of f , 24 samples of f' , 24 samples of f'' ; (c) 36 samples of f , 36 samples of $\mathcal{H}f$; (d) 72 samples of f .

Table 1: Approximated results by using different types of data and different total samples.

$\mu(I^{\mathbf{N}})$	f	$\mathcal{H}f$	f'	f''	δ_1	δ_2
16	16	0	0	0	0.1482×10^1	0.1393×10^1
24	24	0	0	0	0.1067×10^1	0.1055×10^1
32	16	16	0	0	0.9064×10^0	0.7532×10^0
32	32	0	0	0	0.6665×10^0	0.6653×10^0
48	16	0	16	16	0.9066×10^0	0.8955×10^0
48	24	24	0	0	0.2861×10^0	0.2400×10^0
48	48	0	0	0	0.2126×10^0	0.2126×10^0
72	24	0	24	24	0.9973×10^{-1}	0.9947×10^{-1}
72	36	36	0	0	0.3802×10^{-1}	0.3233×10^{-1}
72	72	0	0	0	0.2905×10^{-1}	0.2905×10^{-1}
96	32	0	32	32	0.1130×10^{-1}	0.1129×10^{-1}
96	48	48	0	0	0.4527×10^{-2}	0.3836×10^{-2}
96	96	0	0	0	0.3494×10^{-2}	0.3494×10^{-2}
108	36	0	36	36	0.3803×10^{-2}	0.3802×10^{-2}
108	54	54	0	0	0.1537×10^{-2}	0.1315×10^{-2}
108	108	0	0	0	0.1189×10^{-2}	0.1189×10^{-2}

where $t_p = \frac{2\pi p}{2048}$. Similarly, the relative error for approximating $\mathcal{H}f$ is given by

$$\delta_2 = \left(\sum_{p=0}^{2047} |\mathcal{H}f(t_p) - \mathcal{T}_{\mathbf{N}}\mathcal{H}f(t_p)|^2 \right)^{\frac{1}{2}} \bigg/ \left(\sum_{p=0}^{2047} |\mathcal{H}f(t_p)|^2 \right)^{\frac{1}{2}}.$$

All algorithms of experiments are based on FFT representation (19) and all codes are programmed in Matlab R2016b. It is easy to see that the computational complexity for com-

puting N_{out} number of functional values of $f(t)$ by Eq. (19) is

$$\mathcal{O}(N_{out}ML \log L). \quad (38)$$

If N_{out} is a multiple of L , namely $N_{out} = CL$, then the computational complexity is reduced to $\mathcal{O}((C-1)ML^2 \log L)$. Note that M is the number of data types, meaning that it is usually a small integer.

The approximated results by using different types of data and different total samples are listed in Table 1. The first column $\mu(I^{\mathbf{N}})$ is the total number of samples used in each experiment. The column 2 to 5 are respectively the number of samples of f , $\mathcal{H}f$, f' , f'' used in each experiment. The last two columns are the relative errors for approximating f and $\mathcal{H}f$ respectively. It can be seen that the experimentally obtained relative errors δ_1 and δ_2 tend to 0 as $\mu(I^{\mathbf{N}})$ goes to infinity. Observe that δ_1 and δ_2 are nearly equal in each row of Table 1. This is consistent with the theoretical prediction, since the Fourier coefficients of f and $\mathcal{H}f$ possess the same absolute value for all $n \in \mathbb{Z} \setminus \{0\}$. For fixed $\mu(I^{\mathbf{N}})$, approximating f (or $\mathcal{H}f$) from the samples of f performs slightly better than approximating f from the samples of f along with its Hilbert transform, and approximating f from the samples of f along with its first two order derivatives has the worst performance, as compared with the other two approximations. This result is in agreement with the theoretical error estimation (36). Nevertheless, if the same total samples are used to approximate f (or $\mathcal{H}f$), the fluctuations of relative errors caused by different types of data are not significant. We can see this, for example, from the last three rows of Table 1, the relative errors of approximating from

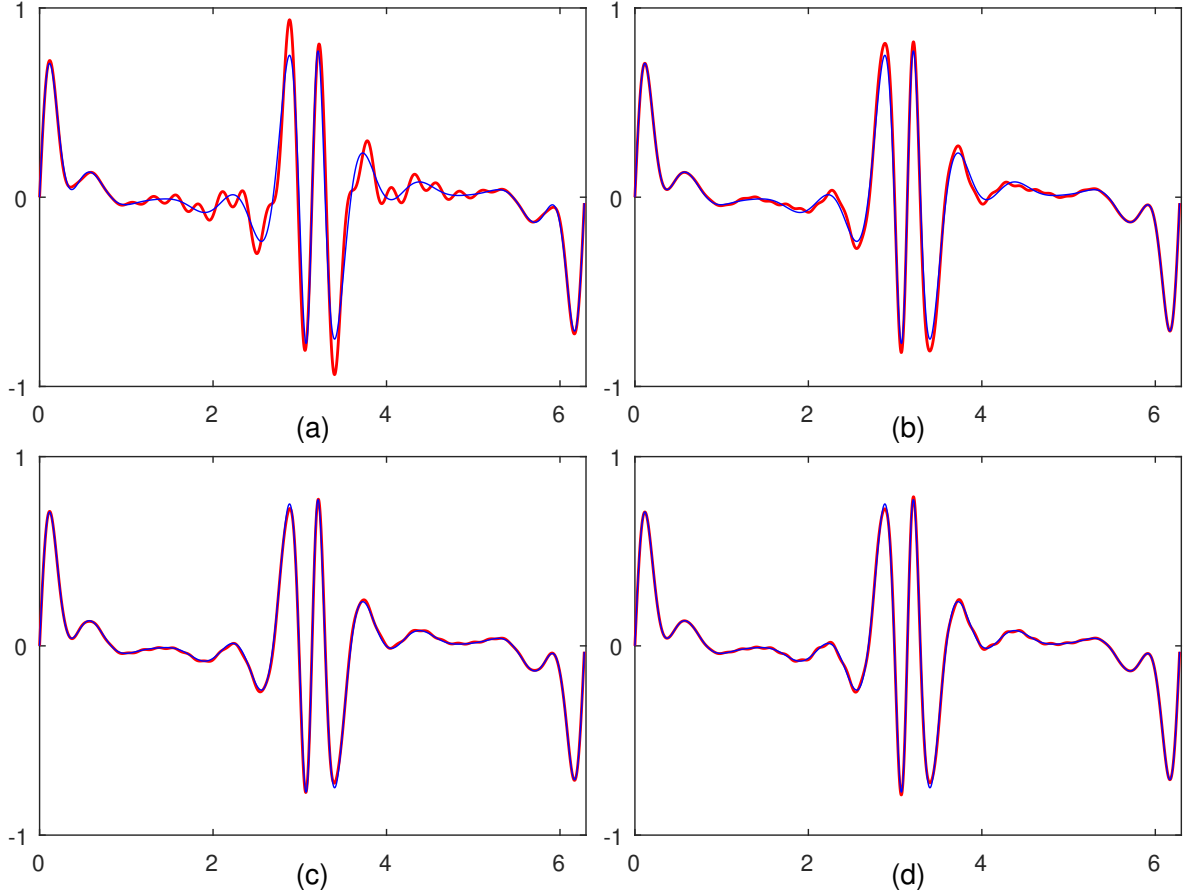


Figure 2: The blue line is the actual $\mathcal{H}f$. The red lines are approximated results for $\mathcal{H}f$ by using (a) 48 samples of f ; (b) 24 samples of f , 24 samples of f' , 24 samples of f'' ; (c) 36 samples of f , 36 samples of $\mathcal{H}f$; (d) 72 samples of f .

different types of data but with same total samples are in the same order. Generally speaking, the total number of samples $\mu(I^{\mathbf{N}})$ is more crucial than the types of samples in approximating signals. Figure 1 and 2 may provide an intuitive reflection for this fact. It can be seen from both figures that the rank of performance in approximation for four experiments is $(a) < (b) < (c) \approx (d)$, where $(a), (b), (c), (d)$ correspond to the experiments of row 7 to 10 in Table 1. It is worth noting that given $\mu(I^{\mathbf{N}}) = LM$ samples associated with f , it is flexible to select $\mathbf{N} = \{N_1, N_2\}$ in $\mathcal{T}_{\mathbf{N}}$ for approximations. If there is some priori information about the frequency of f , we may select \mathbf{N} such that the energy of Fourier coefficients of f is concentrated on $I^{\mathbf{N}}$. Then we can get an optimal approximation which minimizes the relative error.

5.2 Application in image scaling

Image scaling (or resizing) is of importance in many personal, medical and industrial imaging applications [13, 29, 30, 31]. The mainstream image scaling algorithms are based on interpolation [13, 29, 30, 32]. The proposed MIP has a good performance in signal interpolation. In this part, we apply MIP to image scaling problem.

The conventional Shannon sampling theorem [1] and Pappoulis sampling theorem [8] are involved in infinite number of sample values spreading over whole real line and the interpolation functions have infinite duration. Once they are applied to image scaling problem, the truncation errors are inevitable. Fortunately, there is no problem with truncation

error for MIP. Besides, the MIP based image scaling algorithm can preserve lots of information of original image for reshaped image, in view of proposed MIP makes good use of multifaceted information such as first derivative (which may include edge information of image) and second derivative (which may include detail information of image). In addition, simple and fast FFT-based algorithm of MIP also makes proposed method very practical for image scaling.

Our image scaling algorithm is based on Example 2. We first compute interpolation result for each row of image, and then apply interpolation for each column by using the same operations. The derivatives of image are computed by difference method. To evaluate the performance of our method, we are in position to compare the image scaling results of different algorithms by experiments. The scheme of experiments is as follows:

1. Pick the odd (row and column) pixels of original image \mathcal{I} to obtain down scaled image \mathcal{I}_{down} .
2. Scale up \mathcal{I}_{down} by image scaling algorithms such that up scaled image \mathcal{I}_{up} has the same size as \mathcal{I} .
3. Compute relative error $\delta(\mathcal{I}, \mathcal{I}_{up})$, PSNR and correlation coefficient $\eta(\mathcal{I}, \mathcal{I}_{up})$ to evaluate the quality of the up scaled image \mathcal{I}_{up} .

Here, relative error δ , PSNR and correlation coefficient η are commonly used quantitative measurements [13, 29, 31] for evaluating image scaling algorithms. They are defined

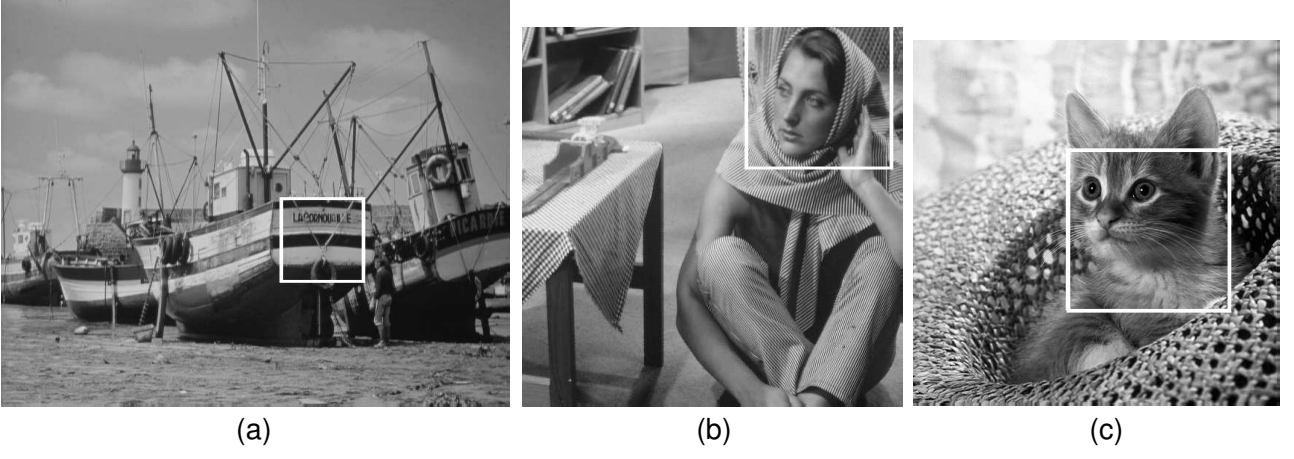


Figure 3: The test images. (a) The boat. (b) Barbara. (c) The cat.

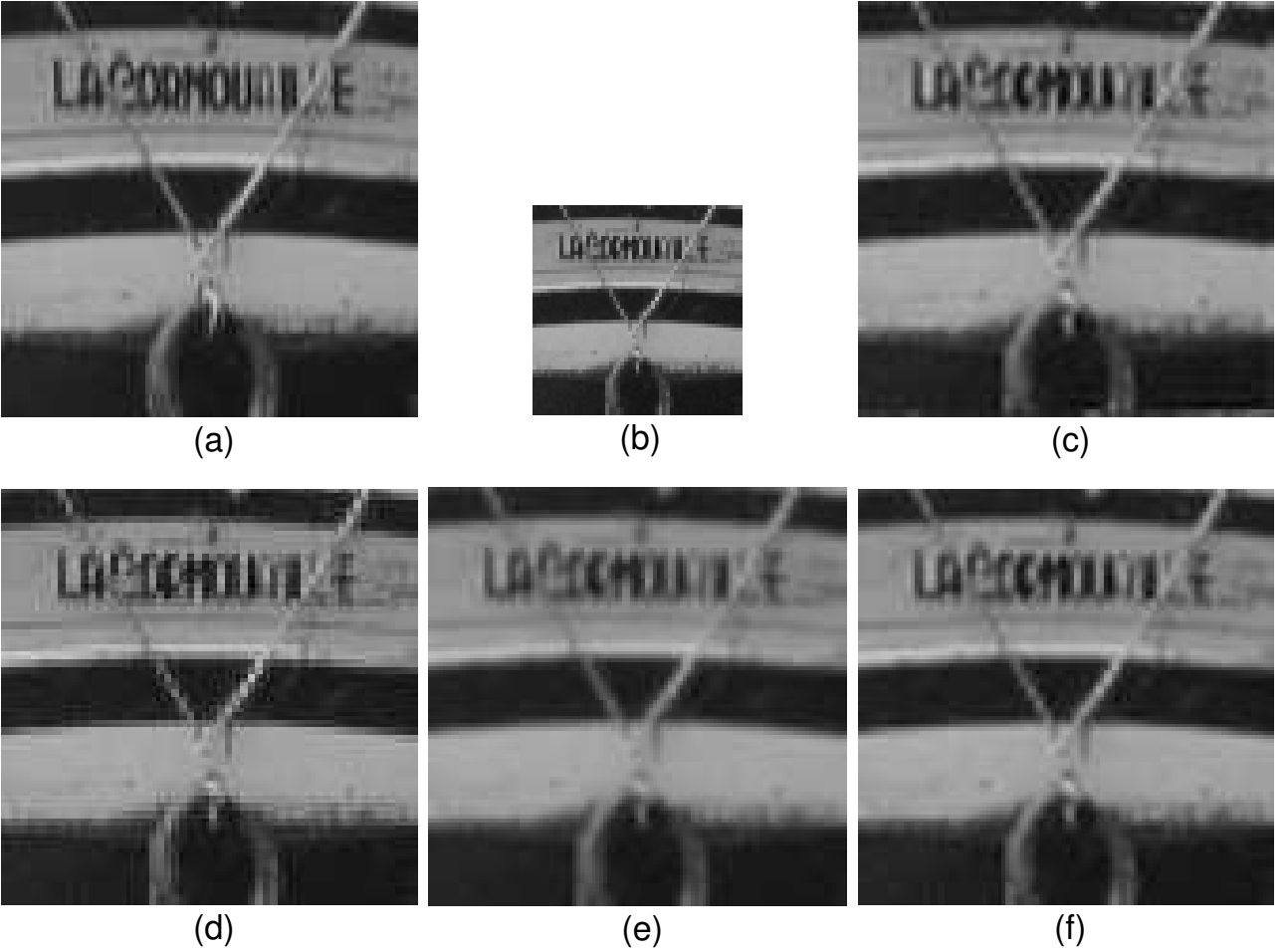


Figure 4: (a) The original (ideal) image of "boat". (b) Down scaled image of (a) by factor 2. (c), (d), (e), (f) are up scaled images by MIP-based, nearest neighbour, bilinear, bicubic algorithms respectively.

respectively as:

$$\delta(\mathcal{I}, \mathcal{I}_{up}) = \frac{\|\mathcal{I} - \mathcal{I}_{up}\|_F}{\|\mathcal{I}\|_F},$$

$$\text{PSNR} = 10 \log_{10} \left(\frac{255^2 \times L_r \times L_c}{\|\mathcal{I} - \mathcal{I}_{up}\|_F^2} \right),$$

$$\eta(\mathcal{I}, \mathcal{I}_{up}) = \frac{\sum_{i,j} (\mathcal{I}(i,j) - \mathcal{I}^0)(\mathcal{I}_{up}(i,j) - \mathcal{I}_{up}^0)}{\|\mathcal{I} - \mathcal{I}^0\|_F \|\mathcal{I}_{up} - \mathcal{I}_{up}^0\|_F},$$

where \mathcal{I}^0 , \mathcal{I}_{up}^0 denote the average pixel values of \mathcal{I} , \mathcal{I}_{up} , and $\|\cdot\|_F$ denotes Frobenius norm, and L_r and L_c are the number of rows and columns of \mathcal{I} respectively.

Table 2: The relative error δ .				
	MIP-based	nearest	bilinear	bicubic
The boat	0.0585	0.1027	0.0806	0.0838
Barbara	0.0597	0.0869	0.0706	0.0739
The cat	0.0643	0.0909	0.0744	0.0768

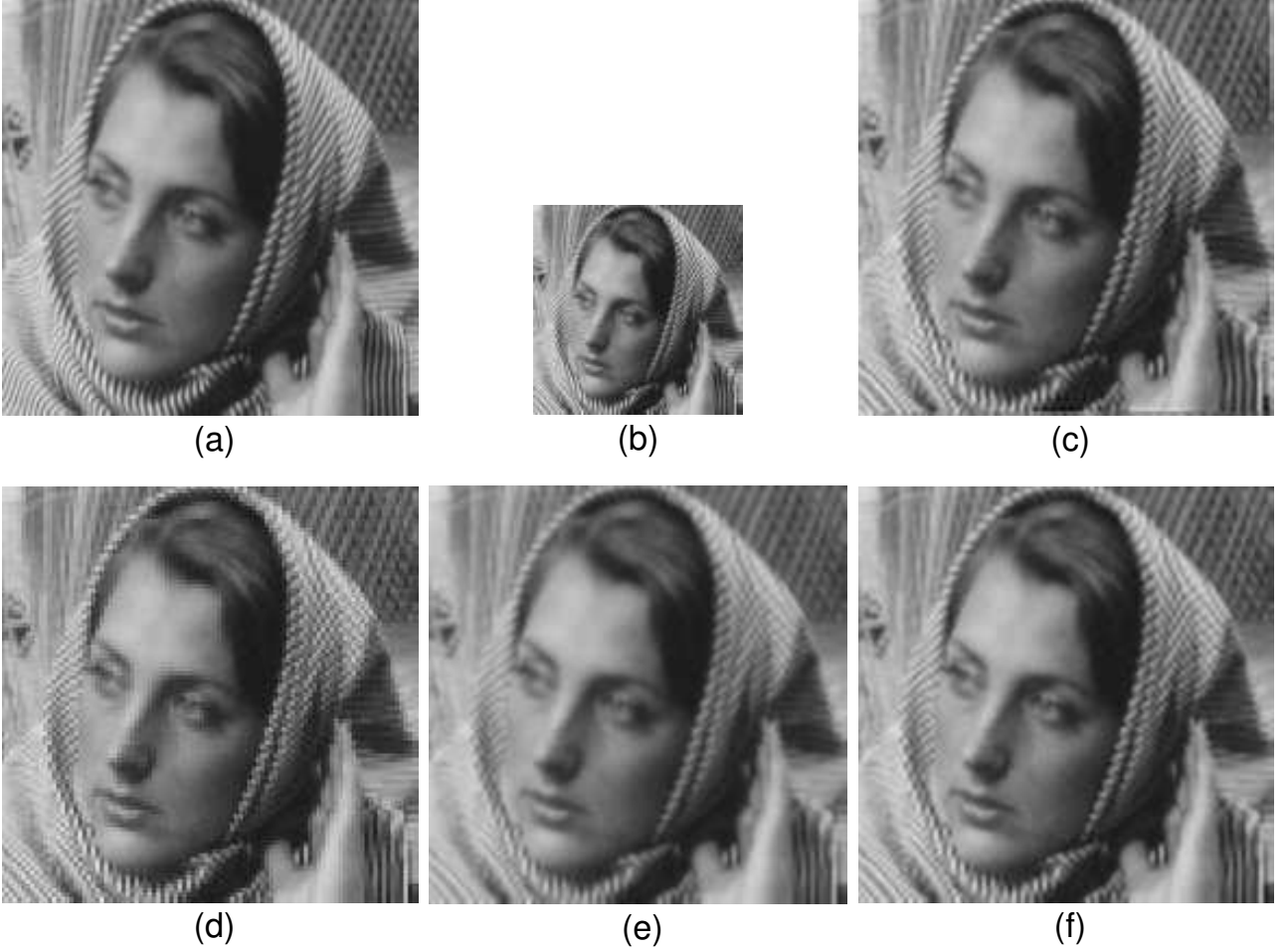


Figure 5: (a) The original (ideal) image of "barbara". (b) Down scaled image of (a) by factor 2. (c), (d), (e), (f) are up scaled images by MIP-based, nearest neighbour, bilinear, bicubic algorithms respectively.

Table 3: The PSNR.

	MIP-based	nearest	bilinear	bicubic
The boat	32.0720	27.1822	29.2796	28.9484
Barbara	30.5528	27.2857	29.0944	28.6967
The cat	31.1380	28.1362	29.8691	29.5975

Table 4: The correlation coefficient η .

	MIP-based	nearest	bilinear	bicubic
The boat	0.9845	0.9578	0.9729	0.9713
Barbara	0.9759	0.9525	0.9679	0.9653
The cat	0.9757	0.9537	0.9683	0.9665

We consider four types of image scaling algorithms: (1) the MIP-based algorithm derived from the previous section; (2) nearest neighbour algorithm; (3) bilinear algorithm; (4) bicubic algorithm. The latter three are popularly used image scaling algorithms and they are included in *imresize* function of Matlab image processing toolbox. Three different types of test images, "boat", "barbara" and "cat", are selected for verifying the effectiveness of proposed MIP-based algorithm. The test images are shown in Figure 3 and the regions remarked by boxes are used for experiments. The MIP-based algorithm is implemented by Eq. (19) which is based on FFT and the computational complexity follows from Eq. (38). The other algorithms are implemented directly by *imresize* function in Matlab.

We show the details of experimental results in Figure 4, 5 and 6. Visibly, our algorithm performs better than the other algorithms. The nearest neighbour algorithm enhances high frequency part so that the scaled images are sharper than other images, but it gives rise to obvious mosaics (see for example, the text of the boat, the eyes of barbara and the cat) due to aliasing. For the bilinear algorithm, it has good low frequency response, but produces significant blur which degrades the image quality. The bicubic algorithm also presents slight blur. Compared with the other three algorithms, the proposed MIP-based algorithm has less blur, good contrast, satisfying edge and detail preserving.

In order to eliminate the subjectivity error produced by the visual results observation and provide a more persuasive evaluation of image scaling algorithm. The quantitative measurements for evaluating the quality of the scaled images are listed in Table 2, 4 and 3. It appears that the MIP-based algorithm yields the smallest relative error and the largest PSNR for each test image. This means that among these scaled images, the one scaled by the MIP-based algorithm has the shortest Euclidean distance from the ideal image. The correlation coefficient reflects by its magnitude the strength of the linear relation between scaled image and ideal image. The closer that the value η is to 1, the better the scaled image quality is. Table 4 shows the correlation coefficient for each test image and each algorithm. It demonstrates the superiority of the MIP-based algorithm

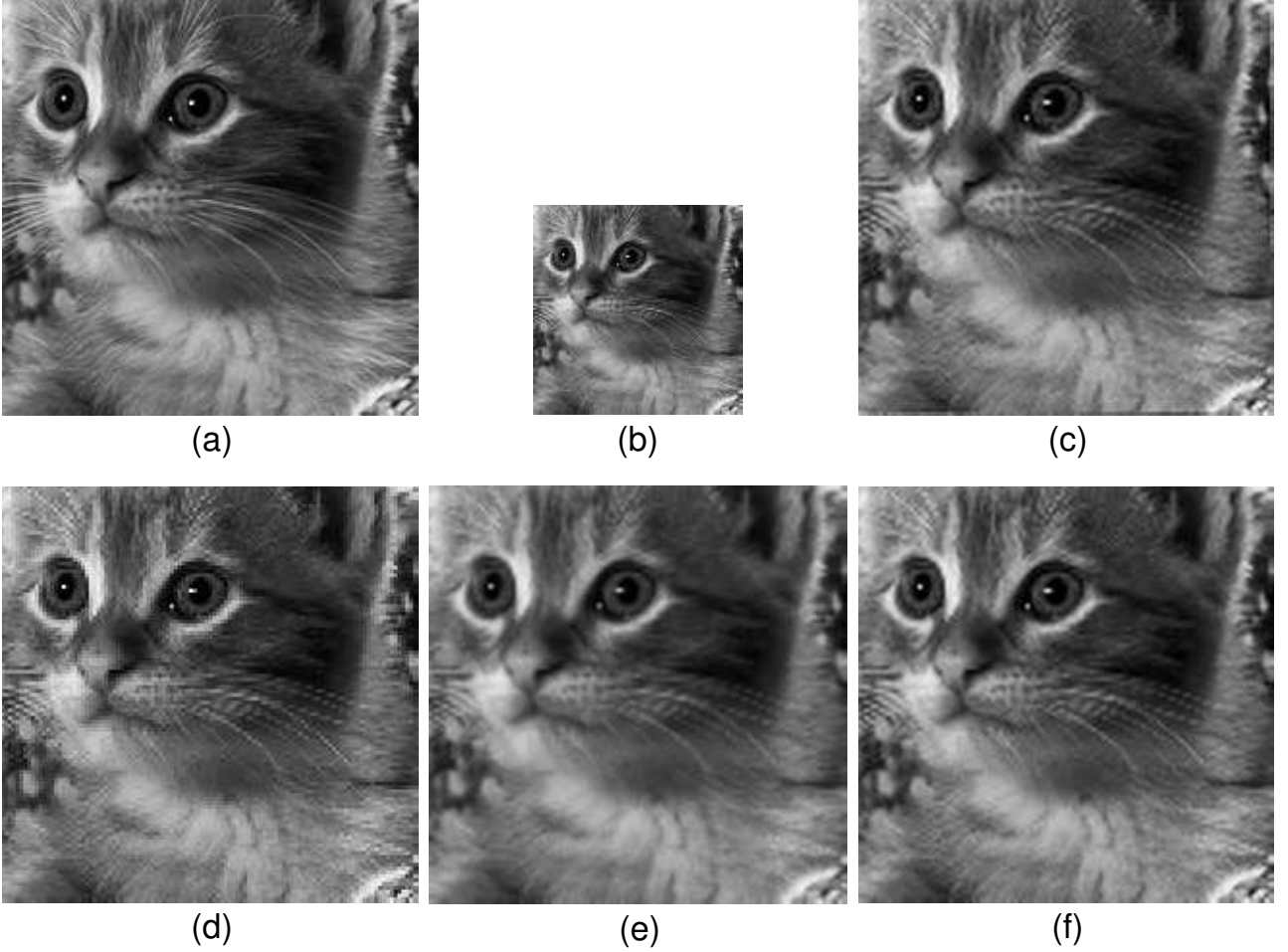


Figure 6: (a) The original (ideal) image of "cat". (b) Down scaled image of (a) by factor 2. (c), (d), (e), (f) are up scaled images by MIP based, nearest neighbour, bilinear, bicubic algorithms respectively.

over nearest neighbour, bilinear and bicubic algorithms.

6 Conclusions

In this paper, we presented a novel multichannel interpolation for periodic signals (MIP). We show that the reconstruction of a continuous periodic signal using data other than the samples of original signal is feasible. Under suitable conditions, only $\mu(I^N)$ total number of samples, no matter what their types, are needed to perfectly recover the periodic signal of the form (4). Quantitative error analysis for non-bandlimited signals is also studied. It is shown that the proposed MIP is an fast and efficient algorithm based on FFT. Both of the theoretical analysis and experiments show that the proposed algorithm can effectively restore the original signal. A particular application is applied for image scaling. Experiments shows visually better image quality than the other conventional image scaling methods. In view of the advantages of the proposed method, a possible direction of our future work is to make this novel interpolation method more widespread and accessible in other applications.

References

- [1] A. I. Zayed, *Advances in Shannon's sampling theory*. CRC press, 1993.
- [2] R. Torres, P. Pellat-Finet, and Y. Torres, "Sampling theorem for fractional bandlimited signals: a self-contained proof. application to digital holography," *IEEE Signal Process. Lett.*, vol. 13, no. 11, pp. 676–679, 2006.
- [3] K. K. Sharma and S. D. Joshi, "Papoulis-like generalized sampling expansions in fractional Fourier domains and their application to superresolution," *Opt. Commun.*, vol. 278, no. 1, pp. 52–59, 2007.
- [4] J. Selva, "Functionally weighted lagrange interpolation of band-limited signals from nonuniform samples," *IEEE Transactions on Signal Processing*, vol. 57, no. 1, pp. 168–181, Jan 2009.
- [5] Y. L. Liu, K. I. Kou, and I. T. Ho, "New sampling formulae for non-bandlimited signals associated with linear canonical transform and nonlinear Fourier atoms," *Signal Processing*, vol. 90, no. 3, pp. 933–945, 2010.
- [6] J. Selva, "FFT interpolation from nonuniform samples lying in a regular grid," *IEEE Transactions on Signal Processing*, vol. 63, no. 11, pp. 2826–2834, June 2015.
- [7] Z. C. Zhang, "Sampling theorem for the short-time linear canonical transform and its applications," *Signal Processing*, vol. 113, pp. 138–146, 2015.

- [8] A. Papoulis, "Generalized sampling expansion," *IEEE Trans. Circuits Syst.*, vol. 24, no. 11, pp. 652–654, 1977.
- [9] K. F. Cheung, "A multidimensional extension of papoulis generalized sampling expansion with the application in minimum density sampling," in *Advanced Topics in Shannon Sampling and Interpolation Theory*. Springer, 1993, pp. 85–119.
- [10] D. Wei, Q. Ran, and Y. Li, "Generalized sampling expansion for bandlimited signals associated with the fractional Fourier transform," *IEEE Signal Process. Lett.*, vol. 17, no. 6, pp. 595–598, 2010.
- [11] —, "Multichannel sampling expansion in the linear canonical transform domain and its application to superresolution," *Optics Communications*, vol. 284, no. 23, pp. 5424–5429, 2011.
- [12] D. Cheng and K. I. Kou, "Generalized sampling expansions associated with quaternion Fourier transform," *Mathematical Methods in the Applied Sciences*, pp. n/a–n/a, mma.4423. [Online]. Available: <http://dx.doi.org/10.1002/mma.4423>
- [13] Y. Li, X. Sha, and D. Wei, "Image scaling algorithm using multichannel sampling in the linear canonical transform domain," *Signal, Image and Video Processing*, vol. 8, no. 2, pp. 197–204, 2014.
- [14] S. Goldman, *Information Theory*. Prentice-Hall, 1953.
- [15] H. Ogawa, "A generalized sampling theorem," *Electronics and Communications in Japan (Part III: Fundamental Electronic Science)*, vol. 72, no. 3, pp. 97–105, 1989.
- [16] T. Schanze, "Sinc interpolation of discrete periodic signals," *IEEE Transactions on Signal Processing*, vol. 43, no. 6, pp. 1502–1503, 1995.
- [17] F. Candocia and J. C. Principe, "Comments on "Sinc interpolation of discrete periodic signals"," *IEEE Transactions on signal processing*, vol. 46, no. 7, pp. 2044–2047, 1998.
- [18] S. R. Dooley and A. K. Nandi, "Notes on the interpolation of discrete periodic signals using sinc function related approaches," *IEEE Transactions on Signal Processing*, vol. 48, no. 4, pp. 1201–1203, 2000.
- [19] M. Jacob, T. Blu, and M. Unser, "Sampling of periodic signals: A quantitative error analysis," *IEEE Transactions on Signal Processing*, vol. 50, no. 5, pp. 1153–1159, 2002.
- [20] E. Margolis and Y. C. Eldar, "Nonuniform sampling of periodic bandlimited signals," *IEEE Transactions on Signal Processing*, vol. 56, no. 7, pp. 2728–2745, 2008.
- [21] L. Xiao and W. Sun, "Sampling theorems for signals periodic in the linear canonical transform domain," *Optics Communications*, vol. 290, pp. 14–18, 2013.
- [22] G. B. Folland, *Fourier analysis and its applications*. American Mathematical Soc., 1992, vol. 4.
- [23] D. Gabor, "Theory of communication. Part 1: The analysis of information," *Journal of the Institution of Electrical Engineers-Part III: Radio and Communication Engineering*, vol. 93, no. 26, pp. 429–441, 1946.
- [24] L. Cohen, *Time-frequency analysis*. Prentice hall, 1995, vol. 778.
- [25] F. W. King, *Hilbert transforms*. Cambridge University Press, 2009.
- [26] Y. Mo, T. Qian, W. Mai, and Q. Chen, "The AFD methods to compute Hilbert transform," *Applied Mathematics Letters*, vol. 45, pp. 18–24, 2015.
- [27] D. Fraser, "Interpolation by the FFT revisited-an experimental investigation," *IEEE Transactions on Acoustics, Speech, and Signal Processing*, vol. 37, no. 5, pp. 665–675, 1989.
- [28] L. Marple, "Computing the discrete-time" analytic" signal via FFT," *IEEE Transactions on signal processing*, vol. 47, no. 9, pp. 2600–2603, 1999.
- [29] T. M. Lehmann, C. Gonner, and K. Spitzer, "Survey: Interpolation methods in medical image processing," *IEEE transactions on medical imaging*, vol. 18, no. 11, pp. 1049–1075, 1999.
- [30] P. Thévenaz, T. Blu, and M. Unser, "Interpolation revisited [medical images application]," *IEEE Transactions on medical imaging*, vol. 19, no. 7, pp. 739–758, 2000.
- [31] S. Battiato, G. Gallo, and F. Stanco, "A locally adaptive zooming algorithm for digital images," *Image and vision computing*, vol. 20, no. 11, pp. 805–812, 2002.
- [32] A. Horé, D. Ziou, and F. Deschênes, "A new image scaling algorithm based on the sampling theorem of papoulis," *Image Analysis and Recognition*, pp. 1–11, 2007.